

p. 1491

XP-000978657

P.D. 1985  
P. 1491-1500 (10)

## ANODIC OXIDATION OF $\beta$ -CYANOETHYL ETHERS

B. WERMECKES and F. BECK

University Duisburg, FB 6, Elektrochemie, Lotharstraße 63, D 4100 Duisburg 1, F.R.G.

(Received 5 February 1985; in revised form 22 April 1985)

**Abstract**—Anodic oxidation of  $\beta$ -cyanoethyl ethers  $R-O-CH_2CH_2CN$  ( $R = Me, Et, t-Bu, CH_2CH_2CN$ ) has been performed in 1.6 M  $H_2SO_4$ , using platinum and lead dioxide as anode materials. The main products were cyanoacetic acid (CEA) and the acid corresponding to  $R$  (formic acid for  $R = Me$ , acetic acid for  $R = Et$ ). In the case of  $R = Et$  (EPN), HAC was found with current efficiencies up to 81% (at low conversions), while CEA was generated with relatively low efficiencies up to 34%.

Kinetic curves for EPN exhibit an early appearance of  $\beta$ -oxypropionitrile (OPN), the intermediate to CEA, and acetaldehyde. Thus, the  $-CH_2$  group of Et is primarily attacked to yield the semiacetal in a two-electron oxidation, which is rapidly cleaved in acid solutions to yield the above-mentioned intermediates. HCN found as a side product is derived from anodic attack at the  $-CH_2$  group adjacent to the cyano group, leading to the readily saponified cyanohydrin.

The ether reacts in the adsorbed state. This leads to large positive potential shifts and unusual Tafel slopes of  $240-300 \text{ mV decade}^{-1}$  due to only partial efficiency of Galvani voltage. Moreover, a partial coverage of Pt electrode with  $PtO_2$  has been detected even in the presence of the ether. Coincidence of  $PtO_2$ -potential and initial oxidation potential of ether leads to the proposal of a mechanism in terms of redox catalysis.

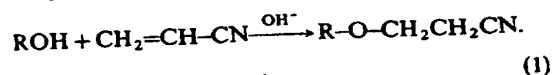
It has been found in addition, that diethyl ether is oxidized to HAC in high yields. Thus, our new findings are not restricted to  $\beta$ -cyanoethyl ethers.

### 1. INTRODUCTION

"Aliphatic ethers are difficult to oxidize" is a statement generally found, even in very recent overviews[1, 2]. However, this is a prejudice. As a consequence, nearly no electrochemical examples can be found in the literature. An early observation, according to which in a mixture of diethylether,  $HClO_4$  and some water, no gas evolution is found at the Pt anode[3], is in contradiction to this. In this way, "the anodic oxidation of aliphatic ethers may be a profitable area for further investigation"[4].

We were able to show that aliphatic ethers are indeed cleaved anodically in high yields to the corresponding carboxylic acids. Some aldehyde was found in addition. Our conditions were quite conventional due to practical reasons, namely diluted aqueous sulfuric acid as an electrolyte and platinum or lead dioxide as positive electrodes. The starting materials were mainly  $\beta$ -cyanoethyl ethers, which are easily synthesized by alkali-catalysed cyanoethylation of the

corresponding alcohols[5]:



Diethyl ether ( $Et_2O$ ) was only used for comparison. The compounds can be also regarded as being derived from propionitrile, and the abbreviations compiled in Table 1 and used in this paper, start from this, eg EPN =  $\beta$ -ethoxypropionitrile.

### 2. EXPERIMENTAL

#### 2.1. Preparative electrolysis

A 250 ml cylindric glass cell with cooling jacket and planar ground cover was used throughout.

The anodes were:

- Bright platinum sheet,  $d = 0.1 \text{ mm}$ , cleaning procedure see[7],  $A = 2 \times 20 \text{ cm}^2$ .

Table 1. Starting materials

No.	Formula	Abbreviation	B.p./°C (760 Torr)
1	$Me-O-CH_2CH_2CN$	MPN	165
2	$Et-O-CH_2CH_2CN$	EPN	173
3	$t-Bu-O-CH_2CH_2CN$	t-BPN	174
4	$Et-O-CH_2-CH(CN)CH_3$	ECPE	184
5	$NCCH_2CH_2-O-CH_2CH_2CN$	CEE	161-162*
6	$Et-O-Et$	$Et_2O$	34.6

\* B.p. at 5 Torr.

Solubility of 1 and 2 in 1-2 M  $H_2SO_4$  is higher than 1 M, while  $Et_2O$  dissolves to about 1 M solutions.

- Lead sheet, 1 mm, anodic formation of  $\text{PbO}_2$  layer in 10%  $\text{H}_2\text{SO}_4$ , 20 h at  $10 \text{ mA cm}^{-2}$ ,  $A = 2 \times 22.5 \text{ cm}^2$ .

The cathodes were two Pt-wire electrodes,  $A = 2 \times 0.3 \text{ cm}^2$ , arranged symmetrically to the anode at a distance of about 1.5 cm. In this way the cell worked as a quasi-divided cell due to the fact that cathodic reconversion of anodic products was strongly diffusion limited.

The electrolyte was 1.6 M  $\text{H}_2\text{SO}_4$ , unless stated otherwise. Starting material was dissolved to make up 1 M solutions (MPN, EPN), 0.4 M (*t*-BPN), 0.65 M (ECPE) or saturated solutions with supernatant ether (CEE,  $\text{Et}_2\text{O}$ ). Electrolysis was performed in stirred solution at constant current density, mostly 30 and  $75 \text{ mA cm}^{-2}$ , with the theoretical charge (theoretical electrochemical conversion = 100% at  $8 \text{ F mol}^{-1}$ ). Typical cell voltages with this cell design were 7–8 V at  $75 \text{ mA cm}^{-2}$  and  $35^\circ\text{C}$ .

Starting materials (EPN, *t*-BPN and ECPE) were prepared by cyanoalkylation of the alcohols ethanol and *t*-butanol by acrylonitrile and ethanol by methacrylonitrile, respectively[5]. CEE was synthesized by cyanoethylation of water[6]. MPN was kindly provided by BASF company, Ludwigshafen.

Further details of the electrochemical preparative part are described in[7].

## 2.2. Product analysis

The electrolysed solutions were analysed directly via HPLC to yield OPN, HAc, CAA,  $\text{HCOOH}$  and CEA with 0.1 N  $\text{H}_2\text{SO}_4$  as eluent.

200  $\mu\text{l}$  of the electrolyte are diluted 1:25 with 0.1 N  $\text{H}_2\text{SO}_4$ . From this, 20  $\mu\text{l}$  were injected and chromatographed at a flow rate of  $2 \text{ ml min}^{-1}$ . Typical retention times were (metal column Knauer,  $l = 25 \text{ cm}$ ,  $d = 0.8 \text{ cm}$ , filled with LiChrosorb RP 18 ( $\text{C}_{18}$  alkane on  $\text{SiO}_2$ ), particle diameter 5  $\mu\text{m}$ ):

$\text{HCOOH}$	5.5 min
CAA	6.0 min
OPN	7.2 min
CEA	7.8 min
HAc	8.6 min.

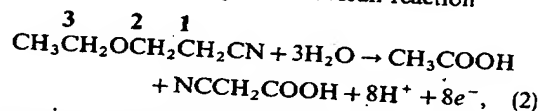
In addition the non-reacted ethers and acetaldehyde could be analysed using  $\text{H}_2\text{O}/\text{MeOH} = 2/1$  as eluent. Detection ensued mainly by refractometry. Details of

the Waters (Rheodyne) Milton Roy-HPLC-setup are given in[7].

Titrimetric control of CEA (after quantitative pre-neutralization of  $\text{H}_2\text{SO}_4$  due to  $\text{p}K_a = 2.44$ ) and HAc was performed with 1 N NaOH (Potentiograph Metrohm). The side product HCN was determined as a step at  $\text{p}K_a = 9.3$ .

After quantitative extraction with  $\text{Et}_2\text{O}$ , gas chromatography (Hewlett Packard 5880A/FID) was used alternatively to determine non-reacted EPN and MPN,  $\text{CH}_3\text{CHO}$  and OPN. It was also possible to measure CEA and HAc quantitatively as methyl esters after reaction with diazomethane.

The yields are calculated in reference to the converted EPN. According to the overall reaction



the main products HAc and CEA can be synthesized theoretically in equimolar quantities to the starting material. Thus, yield is the molar ratio HAc (CEA) found/EPN converted. However, current efficiencies (*ce*) are somewhat undefined due to the branched reaction mechanism, cf Fig. 5. Double counting of charge for the intermediates must be avoided. By this way,  $4 \text{ F mol}^{-1}$  are accounted for each of the main products HAc and CEA.

## 2.3. Electrochemical measurements

A conventional three-electrode setup was used. The cylindrical working electrode was bright Pt,  $A = 0.3 \text{ cm}^2$ . Pretreatment cf[7]. The same electrode was coated with a  $100 \mu\text{m}$   $\text{PbO}_2$  layer[8]. Reference electrode was  $\text{Hg}/\text{Hg}_2\text{SO}_4/1 \text{ M H}_2\text{SO}_4$ . All potentials are recalculated *vs she* (" $U_H$ ").

The electrolyte was stirred magnetically. Voltage scan rates were  $5 \text{ mV s}^{-1}$  for quasi-steady-state curves and  $50\text{--}200 \text{ mV s}^{-1}$  for dynamic curves. Further details see[7].

## 3. RESULTS

### 3.1. Preparative results

The main products in all cases were carboxylic acids. Quantitatively identified were acetic acid HAc, formic

Table 2. Products of anodic oxidation of  $\beta$ -cyanoethyl ethers

Class	Formula	Abbreviation	B.p./ $^\circ\text{C}$ (at 760 Torr)	Analytical method
Main products	$\text{CH}_3\text{COOH}$	HAc	118.1	HPLC, Titration
	$\text{H-COOH}$	—	100.5	HPLC, Titration
	$\text{NC-CH}_2\text{COOH}$	CEA	108*	HPLC, Titration
Side products	$\text{CH}_3\text{-CHO}$	AA	20.8	GC (capillary)
	$\text{H-CHO}^\dagger$	—	—21	—
	$\text{NC-CH}_2\text{CHO}$	CAA	71–72	HPLC, GC
	$\text{NC-CH}_2\text{-CH}_2\text{-OH}$	OPN	230	HPLC, GC
	HCN	—	25.7	Titration

\* B.p. at 0.15 Torr.

† Not analysed quantitatively.

The non-converted starting materials (ethers) were determined quantitatively *via* GC.

Table 3. Anodic oxidation of ethyl- $\beta$ -cyanoethyl ether (EPN) in a 0.16 mole scale ( $c = 1$  M) in 1.6 M aqueous  $H_2SO_4$ . Current conversion  $\beta = 100\%$  corresponds to  $Q = 1.28$  F ( $8$  F  $mol^{-1}$  EPN)

No.	Anode	$j/\text{mA cm}^{-2}$	$T/^{\circ}\text{C}$	$\beta/\%$	Conversion of EPN (analytical)/%	Yield/%*			Current efficiency/%					$\sum ce/\%$	Number of runs
						CEA	HAc	OPN	CEA (4F)	CAA (2F)	HCN (2F)	HAC (4F)			
1	Pt	30	5	100	100	68	90	9	34	1.5	5	46	86.5	2	
2	Pt	75	9	100	99	56	85	11	28	5	5	42	80	3	
3	Pt	30	35	100	100	31	92	40	15	1	6	46	68	2	
4	Pt	75	35	100	100	30	92	42	15	1.5	6	46	68.5	1	
5	Pt	30	35	40	91	0.5	70.5	58	1	2	8.5	81	92.5	1	
6	Pt	30	35	70	98	4	96.5	62.5	3	2	8.5	68	81.5	1	
7 = 3	Pt	30	35	100	100	31	92	40	15	1	6	46	68	2	
8	Pt	30	35	250	100	16	55	0	3	0	2.5	11	16.5	1	
9	PbO <sub>2</sub>	30	5	100	97	59	90	19	29	0.2	4	44	76	1	
10	PbO <sub>2</sub>	62	5	100	95	38	86	16	18	1.5	6	41	66.5	1	
11	PbO <sub>2</sub>	30	35	100	90	8	84.5	32	4	1.0	6	38	49	1	
12	PbO <sub>2</sub>	62	35	100	100	48	83	15	24	1.0	5	42	72	1	

\* Mass yields =  $n_x/n_{EPN}$  (converted)

acid HCOOH and cyanoacetic acid CEA. As side products, the corresponding aldehydes  $CH_3CHO$  and CAA were identified quantitatively. HCN and  $\beta$ -oxypropionitrile (OPN) =  $\beta$ -cyanoethanol were found in addition and analysed quantitatively. In Table 2, the product abbreviations are compiled, together with the methods of quantitative analysis.

The preparative results for EPN as starting material are compiled in Table 3. It can be seen, that HAc is formed at Pt anodes with yields up to 97% and ces up to 81% (at low conversion). The highest values for CEA are somewhat lower, but comparable with data for OPN as the starting material[7]. CAA and HCN are found in smaller quantities as in our former preparations with OPN[7]. A temporary accumulation of the intermediate OPN is found at 35°C relative to 5°C (runs 1-4) and at low conversions (runs 5-8).

The yields with PbO<sub>2</sub> anodes (runs 9-12) are somewhat inferior, quite in accordance with our former findings with OPN[7]. A possible advantage of this electrode material is the low prize and the stability against anodic corrosion due to HCN.

For further kinetic evaluation, the conversion/time curves for starting material EPN, intermediates OPN and CAA and products HAc, HCN and CEA have been monitored in the course of two typical runs, cf Fig. 1. The identity of the results demonstrates that cathodic reduction of organic materials is negligible. Figure 1 shows clearly that OPN and CAA as intermediates are observed nearly from the start, while the end products HAc and especially CEA appear with some delay. The maximum of OPN is attained earlier than the maximum of CAA. Acetaldehyde, not included in Fig. 1, appears simultaneously with OPN at low conversions, but its maximum appears much earlier. The starting material is consumed in the early part of the experiment much faster than in the later periods.

Similar preparative results have been obtained with MPN as a starting material. A characteristic feature which can be found in Table 4 is the presence of formic

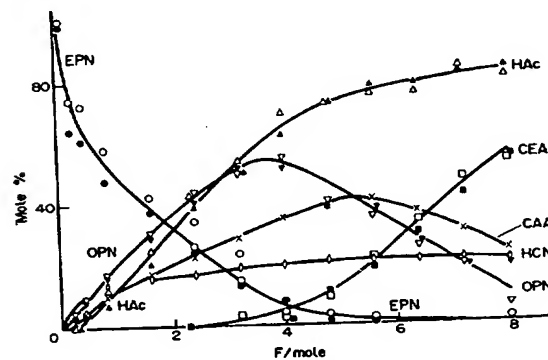


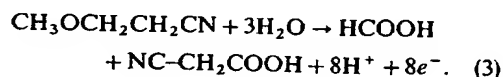
Fig. 1. Conversion/time curves for the anodic oxidation of  $\beta$ -ethoxy propionitrile (EPN),  $n_0 = 137$  mmole, in 1.6 M  $H_2SO_4$  at Pt anodes ( $A = 40\ cm^2$ ) with  $j = 75\ mA\ cm^{-2}$  at 8°C. Empty symbols  $\circ \Delta \square \diamond$ : Run in an undivided cell, cathodes of carbon with the same area as the Pt anode. Filled symbols  $\bullet \blacktriangle \blacksquare \times$ : Run in a quasi-divided cell, as described in section 2.1. Time scale is reduced to F  $mol^{-1}$  (electricity consumed:  $\circ$  EPN (starting material);  $\Delta$  OPN,  $\times$  CAA (intermediates);  $\bullet$  HAc,  $\square$  CEA,  $\diamond$  HCN (products)).

Table 4. Anodic oxidation of methyl- $\beta$ -cyanoethyl ether (MPN) in a 0.16 mole scale ( $c = 1$  M) in 1.6 M aqueous  $H_2SO_4$ . Current conversion  $\beta = 100\%$  corresponds to  $Q = 1.28$  F ( $8$  F mol $^{-1}$  MPN)

No.	Anode	$j/\text{mA cm}^{-2}$	$T/^{\circ}\text{C}$	$\beta/\%$	Conversion of MPN (analytical)/%	Yield/%*			Current efficiency/%					$\sum ce/\%$	Number of runs
						CEA	HCOOH	OPN	CEA (4F)	CAA (2F)	HCN (2F)	HCOOH (4F)			
1	Pt	30	5	100	99.5	60	68	10.5	30	4	6	34	74	1	
2	Pt	30	35	100	100	24	85	26	12	0	5	43	60	2	
3	Pt	30	35	50	85	7	56	73	7	0	9	47.5	63.5	2	
4	PbO <sub>2</sub>	30	5	100	89	57	2	13	25	1	5	0.8	32	1	
5	PbO <sub>2</sub>	30	5	125	92	62	3	9	23	0.5	4	1	28.5	1	
6	PbO <sub>2</sub>	30	35	100	75	41.5	5	25	15.5	0	5	2	22.5	1	
7	PbO <sub>2</sub>	30	35	125	90	40.5	3	18	14.5	0	3	1	18.5	1	
8	PbO <sub>2</sub>	70	35	100	76	53.5	5	18	20.5	0.5	4	3	28	1	

\* Mass yield =  $n_x/n_{\text{MPN, converted}}$

acid instead of acetic acid (case EPN) as one of the two main products. This follows from the overall reaction:



As before,  $ce$  for each of the carboxylic acids have been calculated with an assumed theoretical value of  $4$  F mol $^{-1}$  acid, cf Table 4. Rather low yields and  $ces$  have been found for HCOOH due to its further oxidation to  $\text{CO}_2$ . The dependencies on  $T$ ,  $j$  and  $\beta$  are similar to those for EPN. All values for yields and  $ces$  are somewhat lower than with EPN.

Some other aliphatic ethers have been oxidized anodically. Tertiary butyl- $\beta$ -cyanoethyl ether  $t$ -BPN was used to check the presence of an unattackable alkyl group. An amount of  $t$ -BPN, corresponding to  $0.4$  M, was dispersed in  $1.6$  M  $\text{H}_2\text{SO}_4$ . Electrolysis was performed at  $30$  mA cm $^{-2}$  and  $5^\circ\text{C}$  at Pt under vigorous stirring. The starting material "dissolved" in the course of electrolysis. After  $4$  F mol $^{-1}$  ether, analysis gave a yield and  $ce$  for CEA of  $56\%$ , that for HCN was  $11\%$ . This is much more CEA than with EPN at  $50\%$  conversion, cf Table 3.

Electrolysis with ethyl- $\beta$ -cyanopropyl ether ECPE dissolved with a concentration of  $0.65$  M in  $1.6$  M  $\text{H}_2\text{SO}_4$  (primarily only partially dissolved) at  $30$  mA cm $^{-2}$  and  $35^\circ\text{C}$  at Pt under vigorous stirring gave after consumption of  $8$  F mol $^{-1}$ :

- HAC,  $ce$   $50\%$
- 2-cyanopropionic acid,  $\text{CH}_3\text{CH}(\text{CN})\text{COOH}$ ,  $pK$   $2.9$ ,  $ce$   $10\%$
- HCN,  $ce$   $6\%$
- 2-cyanopropanol was identified qualitatively by GC.

Bis- $\beta$ -cyanoethyl ether CEE, which is easily available from acrylonitrile and water, was electrolysed under various conditions initially present as an emulsion in rapidly stirred  $1.6$  M  $\text{H}_2\text{SO}_4$ . The oil "dissolved" in the course of electrolysis. The results are compiled in Table 5.

For comparison  $\text{Et}_2\text{O}$  (diethyl ether) was electrolysed under the same conditions at Pt with  $j = 75$  mA cm $^{-2}$ . The starting material was in about 10-fold excess at the beginning of the electrolysis, and an emulsion was processed throughout the experiment. Acetaldehyde (AA) as a volatile product was extracted after electrolysis with excess ether in 20 steps at room temperature rather than by continuous extraction with distillative recycling of ether. The results in terms of current efficiency after  $8$  F mol $^{-1}$  ether were [run (1) at  $12^\circ\text{C}$ , run (2) at  $35^\circ\text{C}$ ]:

Product HAC (4F) (1)  $ce$   $55\%$  (2)  $ce$   $69\%$   
 Product  $\text{CH}_3\text{CHO}$  (2F) (1)  $ce$   $15\%$  (2)  $ce$   $4\%$ .

Analytical HAC results via HPLC and titration were in good agreement. However, direct analysis of the electrolyte for AA by HPLC led to a threefold value for  $ce$  and not to a fraction of the  $ce$  determined after exhaustive extraction via GC. This certainly is due to losses of AA during the extraction. Thus, the acetaldehyde values given above can be regarded as a lower limit.

All results presented hitherto were obtained in  $1.6$  M  $\text{H}_2\text{SO}_4$ . EPN was investigated in addition at

Table 5. Anodic oxidation of *bis*- $\beta$ -cyanoethyl ether (CEE) in 1.6 M  $\text{H}_2\text{SO}_4$ ,  $8 \text{ F mol}^{-1}$ ,  $j = 30 \text{ mA cm}^{-2}$ 

No.	Anode	$c(\text{CEE})/\text{M}$	$T/^\circ\text{C}$	Current efficiency/%				$\sum ce/\%$
				CEA (4F)	CAA (2F)	OPN*	HCN (2F)	
1	Pt	1	5	40	4.5	40	13.5	58
2	Pt	1	35	34	—†	—†	13	>47
3	$\text{PbO}_2$	1	5	39	7	43	10	56

\* Material yield/%.

† Not analysed.

Table 6. Anodic oxidation of EPN (No. 1 and 2) and OPN (No. 3) at  $35^\circ\text{C}$  on Pt anodes at higher pH values,  $\beta = 100\%$  (8 and  $4 \text{ F mol}^{-1}$ , respectively)

No.	pH	$j/\text{mA cm}^{-2}$	$\beta/\%$ (analytical)	Yield/%			Current efficiency/%			
				CEA	HAc	OPN	CEA	CAA	HAc	HCN
1	3	30	91.5	0	72	40	0	1	33	8
2	6	75	100	0	70	38	0	1	35	3.5
3	6	75	61	1.5	—	—	1	0.5	—	18

higher pH (pH 3 and 6). For pH 6, a buffered electrolyte  $1.5 \text{ M Na}_2\text{SO}_4 + 0.2 \text{ M KH}_2\text{PO}_4 + \text{NaOH}$  up to pH 6 was used. The run at pH 3 was performed in unbuffered  $1.5 \text{ M Na}_2\text{SO}_4$ , slightly acidified with  $\text{H}_2\text{SO}_4$ . In both cases, pH was measured in the course of electrolysis by a glass electrode, and controlled by addition of NaOH.

In Table 6, the preparative results are compiled. Contrary to acid conditions, hardly any CEA has been found, and HAc formation was less efficient. HCN is found as before. OPN as a starting material yields nearly no CEA or CAA, but it is attacked at the other  $-\text{CH}_2$  group to give HCN to an appreciable extent.

### 3.2. Electrochemical measurements

Preparative results have been supplemented by electrochemical measurements. Figure 2 shows quasi-steady-state current-voltage curves at platinum in a Tafel plot for ethers EPN and MPN, the intermediate OPN and the basic curve.  $\text{Et}_2\text{O}$  and propionitrile are shown for comparison. Concentrations of depolarizers were 1 M. The curves measured in the presence of compounds containing the nitrile group are strongly shifted in the positive direction, as we have observed formerly [7, 9].

Tafel slopes for cyanoethyl ether oxidation are usually high,  $b = 250\text{--}300 \text{ mV decade}^{-1}$ . Slightly S-shaped curves are obtained rather than Tafel lines. An appreciable hysteresis is observed on sweep reversal at a scan rate  $v_s = 5 \text{ mV s}^{-1}$ . The decreasing branch was more positive, and it was used for replotting in the Tafel diagram.

The strong potential shifts for 0.1 M solutions are collected in Table 7, demonstrating again the very pronounced effect.

Contrary to Pt, at  $\text{PbO}_2$ -anodes current-voltage

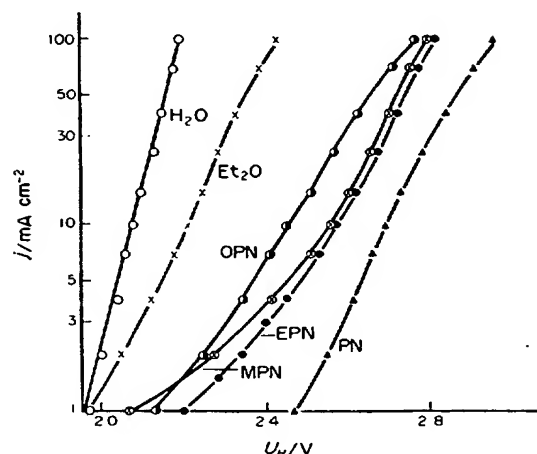
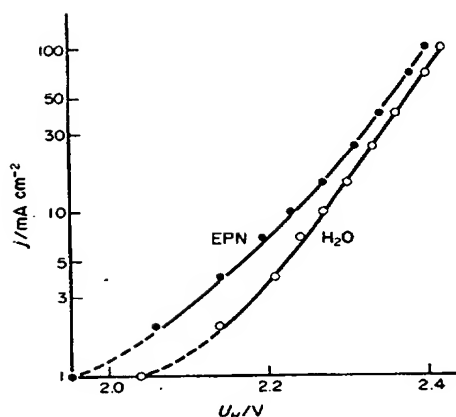
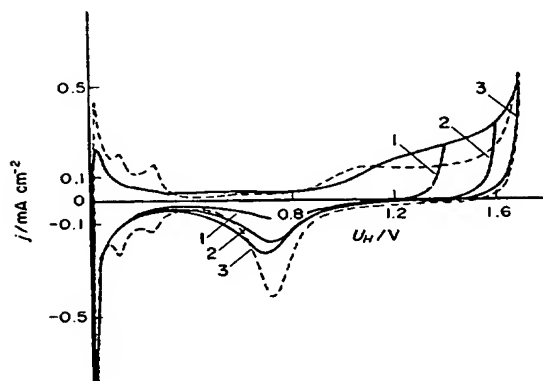


Fig. 2. Tafel plots for the anodic oxidation of nitrile group containing compounds on Pt electrodes in  $1.0 \text{ M H}_2\text{SO}_4$  at  $20^\circ\text{C}$  in stirred solutions. Voltage scan rate  $5 \text{ mV s}^{-1}$ . The branch for negative voltage scan direction has been evaluated:  $\circ$ — $\circ$  basic curve;  $\bullet$ — $\bullet$  1 M EPN;  $\circ$ — $\circ$  1 M MPN;  $\bullet$ — $\bullet$  1 M OPN;  $\blacktriangle$ — $\blacktriangle$  1 M propionitrile;  $\times$ — $\times$   $\text{Et}_2\text{O}$ , sat. ( $\sim 1 \text{ M}$ ) for comparison.

curves in the presence of nitrile compounds coincide nearly with the base curve, cf Table 6. In a few cases even a slight depolarization is observed (negative sign in the table). No hysteresis is observed. As is shown in Fig. 3, a nearly normal slope of  $140 \text{ mV decade}^{-1}$  is found for both Tafel lines at high current densities. Cyclic voltammetric curves on Pt in  $1.0 \text{ M H}_2\text{SO}_4$  ( $v_s = 100 \text{ mV s}^{-1}$ ) are shown in Fig. 4. The basic curve shows the common regions of  $\text{H}_{\text{ad}}$  formation and

Table 7. Potential shifts (V) for anodic oxidation of cyanocompounds in reference to the basic curve in 1.0 M H<sub>2</sub>SO<sub>4</sub>. Concentration in all cases 0.1 M

No.	Depolarizer	Pt anode cd/mA cm <sup>-2</sup>				PbO <sub>2</sub> anode cd/mA cm <sup>-2</sup>
		3	10	30	100	
1	CH <sub>3</sub> CN, AcN	0.28	0.38	0.42	0.49	0.01
2	C <sub>2</sub> H <sub>5</sub> CN, PN	0.26	0.39	0.46	0.54	0.03
3	CH <sub>2</sub> =CHCN, AN	0.54	0.65	0.72	0.78	0
4	OPN	0.18	0.31	0.39	0.48	-0.01
5	MPN	0.25	0.37	0.45	0.53	0.04
6	EPN	0.26	0.33	0.41	0.49	-0.01
7	ECPE	0.20	0.33	0.45	0.50	-0.01

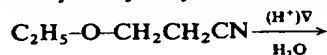
Fig. 3. Tafel plots for the anodic oxidation of EPN on PbO<sub>2</sub> electrodes in 1.0 M H<sub>2</sub>SO<sub>4</sub> at 20°C in stirred solutions,  $v_s = 5 \text{ mV s}^{-1}$ .Fig. 4. Cyclic voltammetry on Pt electrodes in 1.0 M H<sub>2</sub>SO<sub>4</sub>. Voltage scan rate  $v_s = 100 \text{ mV s}^{-1}$ . Variation of potential of positive scan reversal ——— basic curve; ——— curve in the presence of 1 M EPN, voltages of scan reversal ( $U_H$ ) (1) 1.4 V, (2) 1.6 V, (3) 1.7 V. Shown is the sixth cycle after starting the experimental sequence. Freshly prepared Pt electrode for the first sequence at the most positive potential of scan reversal.  $T = 20^\circ\text{C}$ , N<sub>2</sub> purging.

dissolution at negative potentials, double layer charging at medium potentials and oxide layer built up at positive potentials. The voltammogram is distinctly modified in the presence of 1 M EPN as an example; current grows rapidly in the oxide layer region, and oxide reduction peak, detected in the reverse scan direction, is appreciably lessened. Moreover,  $H_{ad}$  peaks disappear nearly completely.

#### 4. DISCUSSION

##### 4.1. Nature of starting material

We have found that anodic oxidation of cyanoethyl ethers at Pt or PbO<sub>2</sub> anodes, in aqueous H<sub>2</sub>SO<sub>4</sub> led to the carboxylic acid corresponding to the alkyl or cyanoalkyl groups, in high yields and current efficiencies, cf Equations (2) and (3). Analogous to this, diethyl ether, investigated for comparison, yielded acetic acid with high efficiency. Thus, the anodic reaction is not unique to cyanoethyl ethers. Carboxylic acids as the most prominent product can only be generated by cleavage of the C—O bond. This poses the question, if this cleavage occurs chemically *via* an acid-catalysed hydrolysis of the ether bond, *eg* for EPN



The alcohols, formed by this way, should be easily oxidizable.

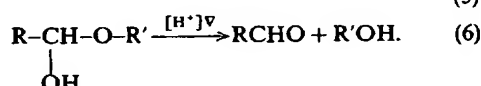
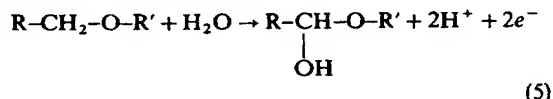
To rule out this triviality, we have stirred the electrolyte, containing 1.6 M H<sub>2</sub>SO<sub>4</sub> and 1.0 M EPN, for 24 h at room temperature. Thereafter, it was extracted exhaustively with ether for another 24-h period. Gas chromatography exhibited 100% starting material EPN. However, to obtain further security, the possibility, that reaction (4) occurs, but that it is shifted back to the left side in the ether solution due to relatively low water activity, was not to be excluded *a priori*. We have performed a second experiment, where 1 M EtOH and 1 M OPN, the products at the right side of Equation (4), were dissolved in 1.6 M H<sub>2</sub>SO<sub>4</sub>. This system was extracted again for 24 h with ether. However, no EPN was detectable *via* GC, but 100% recovery of OPN.

These results prove clearly, that cleavage of C—O bond proceeds *electrochemically*, either directly or

after anodic conversion to reactive intermediate. Direct cleavage after a single electron transfer, yielding a radical and a cation, is believed to be improbable.

#### 4.2. Primary anodic attack

Site of anodic attack of the organic molecule is governed by electron density  $\delta^-$ . In EPN,  $\text{CH}_2$  group No. 3 [for numbering see Fig. 5 and Equation (2)] has the highest  $\delta^-$  due to ether oxygen and methyl group neighbourhood (hyperconjugation effect of methyl group). Methylene group No. 2 has the second highest  $\delta^-$ . In both cases, primary anodic attack leads to a semi-acetal as an intermediate, which is very rapidly cleaved in acid solution [10, 11]:



Thus, anodic attack at  $\text{CH}_2$  group No. 3 leads to acetaldehyde and OPN, while  $\text{CH}_2$  group No. 2 yields cyanoacetaldehyde CAA and EtOH, cf Fig. 6. As the rate constant of acetaldehyde diethylacetal cleavage at  $25^\circ\text{C}$  and pH 1 is as high as  $50 \text{ s}^{-1}$  [12, 13], the rate for semi-acetal cleavage [Equation (6)] must be even higher. A further oxidation of ether molecule to the ester ( $4 \text{ F mol}^{-1}$ ) or even to acid anhydride ( $8 \text{ F mol}^{-1}$ ) prior to hydrolysis can be ruled out for these reasons.

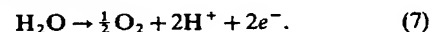
Moreover, product distribution and conversion curve is fully compatible only with anodic oxidation to the semi-acetals with  $2 \text{ F mol}^{-1}$ , and immediate subsequent solvolytic cleavage.

Distinguished features of current-voltage curves at platinum are strong positive shift of potentials in the

presence of organic compounds as well as unusual "flat" Tafel slope, cf Figs 2 and 3 and Table 7. Both findings are indicative of strong adsorption of the depolarizer molecules at the platinum surface. Potential shifts are not simply due to  $i_r$  drop in an adsorption layer [7]. Galvanostatic transients reveal only a specific resistance of  $0.2\text{--}0.3 \text{ ohm cm}^2$ , which is not in accordance with our former interpretation [7]. Cyclic voltammetric curves with Pt anodes (Fig. 4) reveal an appreciable decrease of surface coverage for oxide in the presence of organic molecules. Basic curve behaviour in diluted  $\text{H}_2\text{SO}_4$  is well established in the literature [14, 15]. A quantitative evaluation of surface charges  $Q_A$  involved in the anodic charge positive to  $U_H = 0.8 \text{ V}$  and the cathodic oxide reduction peak at  $U_H \approx 0.7 \text{ V}$  is given in Fig. 6. The basic curve is in good agreement with results of Peuckert *et al.*, performed at a Pt single crystal with a larger roughness factor [15]. The  $Q_A$  values in the presence of the strongly adsorbed organic compounds are larger for the anodic sweep and smaller for the cathodic. Similar curves have been observed for electrosorption of benzene [17, 18] and of benzoic acid [19] on Pt, respectively.

Impedance measurements (Zahner IM5e) of galvanostatically polarized Pt anode show a 10-fold decrease of capacity and a threefold increase of resistivity in the presence of EPN.

These results lead us to the conclusion that both species, organic and oxide, are present at the electrode surface in the course of electrolysis, as it is schematically shown in Fig. 7. The organic molecules occupy active sites at the "edge" of oxide layers for anodic oxygen evolution [20]:



Thus, this reaction is nearly completely suppressed. At that stage, the primary oxidation to the semi-acetal may proceed according to Equation (5), but a mechanism *via* heterogeneous redox catalysis [21] with PtO

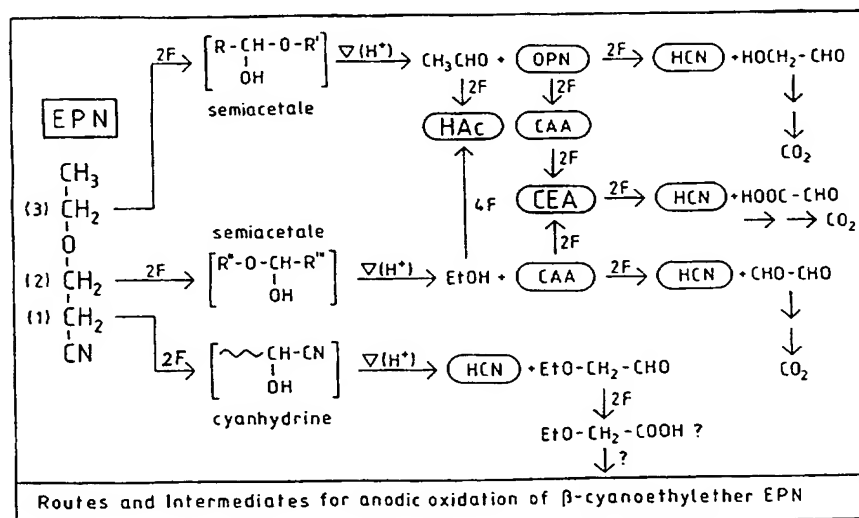


Fig. 5. Proposed reaction mechanism for the anodic oxidation of  $\beta$ -cyanoethyl ether EPN to the main products HAC and CEA.

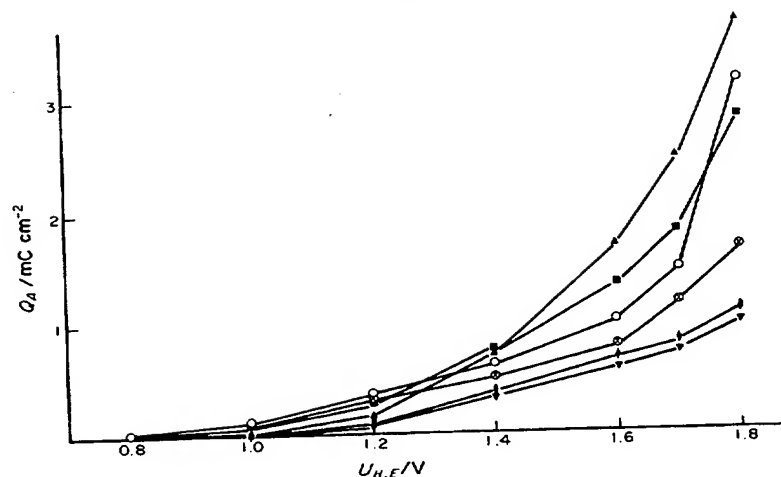


Fig. 6. Plot of surface specific charge  $Q_A$  derived from experiments according to Fig. 4 vs potential of positive scan reversal:  $\circ, \bullet$  basic curve, anodic and cathodic;  $\blacktriangle, \blacktriangledown$  1 M OPN, anodic and cathodic;  $\blacksquare, \blacklozenge$  1 M EPN, anodic and cathodic.

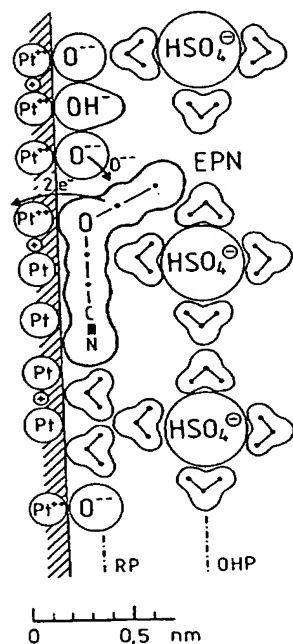
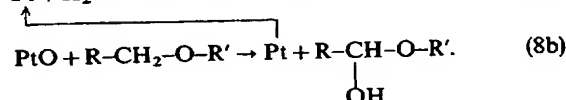
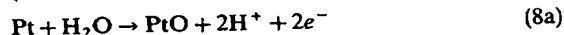


Fig. 7. Schematic representation of double layer structure at a platinum anode for anodic oxidation of EPN.

(or  $\text{PtO}_2$ ) as the oxidant cannot be ruled out:



This mechanism is involved in Fig. 7. A very strong indication for this kind of mechanism is presented by Fig. 4, where current rise for oxide formation and

current voltage curve in the presence of EPN coincide nearly. Similar phenomena are observed for  $\text{NiOOH}$ [22, 23],  $\text{PbO}_2$ [24, 25] and  $\text{CrO}_3$ [21]. On the other hand,  $\text{PbO}_2$  cannot be operative in terms of heterogeneous redox catalysis in our case, for oxidation potentials are much more positive than  $\text{Pb}^{2/4}$  redox couple, cf Fig. 4. If electron transfer proceeds directly from a reaction plane RP (cf Fig. 7), only a fraction  $f$  of the total Galvani voltage  $\Delta\phi$  is operative at that point. For a symmetrical potential barrier between surface and RP, 50% of  $f\Delta\phi$  modifies this barrier. By this way, for constant concentrations, rate of anodic process is given by

$$j = K \exp\left(\frac{1}{2} f \Delta\phi F / RT\right), \quad (9)$$

assuming single electron transfer in the rate-determining step. The Tafel slope

$$b = \frac{d(U_H)}{d \log j} = 2.30 \frac{2 RT}{f F} \quad (10)$$

is derived from this ( $U_H$  = potential vs she). For  $f = 0.5-0.4$ ,  $b = 240-300 \text{ mV decade}^{-1}$  are obtained, as observed.

Cell voltage was very stable in the course of preparative runs. Potential-time curve for galvanostatic polarization of Pt anodes in the presence of EPN reveals a remarkably constant electrode potential for hours. This is quite contrary to the anodic conversion of nitrile in non-aqueous electrolytes, where "passivation" or filming of the anode is notorious[16].

#### 4.3. Further reactions

After cleavage of the semi-acetal, very reactive intermediates as alcohols and aldehydes appear in the electrolyte, which are oxidized further. In the case of EPN on Pt anodes, OPN appears very early, accompanied by acetaldehyde (not shown in Fig. 1), and acetic acid is observed subsequently.

This underlines our mechanism, according to which  $-\text{CH}_2$  group No. 3 is attacked mainly, yielding



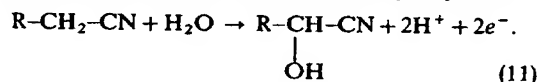
Table 8. Comparison of yields of CEA (and HAc) via anodic ether oxidation, Pt anode, 1.6 M  $\text{H}_2\text{SO}_4$ , 75  $\text{mA cm}^{-2}$ , 35°C

Starting material	$\beta/\text{F mol}^{-1}$	CEA		HAc	
		yield/%	ce/%	yield/%	ce/%
EPN	8	30	15	92	46
MPN*	8	24	12	—	—
tBPN†	4	56	56	—	—
ECPE	8	—	—	—	50
CEE*	8	—	34	—	—
$\text{Et}_2\text{O}$	8	—	—	—	69
OPN (from[7])	4	56	45	—	—
OPN† (from[7])	4	64	62	—	—

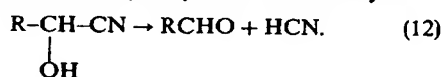
\* 30  $\text{mA cm}^{-2}$ .† 30  $\text{mA cm}^{-2}$ , 5°C.

acetaldehyde- $\beta$ -cyanoethyl semi-acetal, which cleaves immediately to acetaldehyde and OPN.  $\text{CH}_3\text{CHO}$  is rapidly oxidized to HAc. The further oxidation of OPN via CAA to CEA is much more hindered, as seen from the kinetic curves for this three species (cf Fig. 1).

Preparative results, *eg* sequence of conversion runs No. 5–8 in Table 3 are in full agreement with the kinetic curves. Anodic attack at  $-\text{CH}_2$  group No. 1 is not favoured, but nevertheless it proceeds to some extent. The primary intermediate is a cyanhydrine



This is again rapidly hydrolysed *via* acid catalysis:

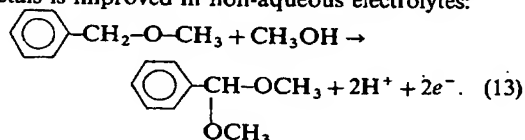


HCN as a product has been analysed. The sources for HCN can be EPN as well as OPN, CAA and CEA, cf Fig. 5. The late appearance of CEA and its sensitivity to further oxidation at  $-\text{CH}_2$  group No. 1 disfavors its yield in comparison to HAc. The early saturation of HCN formation found in Fig. 1 is somewhat unclear and contradicts this view as well as the relatively high yields for HCN formation *via* OPN found formerly[7].

#### 4.4. Comparison to results in non-aqueous electrolytes

For the first time we have performed with this study a systematic investigation of anodic behaviour of aliphatic ethers. As pointed out in the introduction, anodic inertness of these compounds could not be confirmed.

Some work has been published concerning anodic oxidation of benzylic ethers in non-aqueous electrolytes, namely methanol/ $\text{NaOCH}_3$ [26] and moist acetonitrile[27–29]. Acetals and semi-acetals have been found as typical intermediates or products. Stability of acetals is improved in non-aqueous electrolytes:



Hydroquinonedimethyl ether has been oxidized to quinone[30]. Dioxane could be converted to the corresponding methoxylation product[31].

#### 4.5. Preparative evaluation

From a preparative point of view, the anodic synthesis of cyanoacetic acid originating from the cyanoethyl group could be of some interest. In Table 8, our results are crosschecked in this regard, showing relatively poor selectivity for this product with the exception of *t*-BPN due to a stabilization of alkyl group. However, OPN as a starting material leads even to an improved selectivity for CEA and is more readily available.

Even diethylether is cleaved anodically to acetic acid in high yields. This has some impact in its application as a solvent for extraction. The electrolyte, saturated with ether and recycled to the cell could be subject to anodic side reactions. Ether as an aprotic solvent has a very limited anodic stability.

The formation of CEA is linked to acid electrolytes. At higher pH values, pH 3 and 6, nearly no CEA could be detected with EPN as a starting material. This pH effect is obscure at the present state.

**Acknowledgements**—Financial support for the HPLC equipment by Deutsche Forschungsgemeinschaft is gratefully acknowledged. We thank BASF company for provision of MPN and Dr H. Krohn of this laboratory for kind assistance in the field of electrochemical measurements.

#### REFERENCES

- O. Hammerich, in *Organic Electrochemistry* (Edited by M. M. Baizer and H. Lund). Marcel Dekker, New York (1983).
- V. D. Parker *et al.*, in *Encyclopedia of Electrochemistry of the Elements*, Vol. XI (Edited by A. J. Bard and H. Lund). Marcel Dekker, New York (1978).
- C. Marie and G. Lejeune, *An. R. Soc. esp. Fis. Quim.* **27**, 447 (1929), cf. *C.A.* **24**, 25 (1930).
- S. D. Ross, M. Finkelstein and E. Rudd, *Anodic Oxidation*. Academic Press, New York (1975).
- A. Bruson, *Org. React.* **5**, 97–106, 111–112 and 131–135 (1949).

6. H. A. Bruson and T. W. Riener, *J. Am. chem. Soc.* **65**, 26 (1943).
7. B. Wermeckes and F. Beck, *Chem. Ber.*, in press.
8. F. Beck, *Elektroorganische Chemie*. Verlag Chemie, Weinheim (1974).
9. F. Beck, *J. appl. Electrochem.* **2**, 59 (1972).
10. P. M. Leininger and M. Kilpatrick, *J. Am. chem. Soc.* **61**, 2510 (1939).
11. S. A. Barker and E. J. Bourne, *J. chem. Soc.* 905 (1952); *Adv. Carbohydr. Chem.* **7**, 137-207 (1952).
12. S. Skrabal and A. Schiffer, *Z. phys. Chem.* **99**, 296 (1921).
13. A. Skrabal, *Z. phys. Chem.* **111**, 98 (1924).
14. S. Gilman, in *Electroanalytical Chemistry* (Edited by A. J. Bard), Vol. 2, pp. 112-192. Marcel Dekker, New York (1967).
15. M. Peuckert, F. P. Coenen and H. P. Bonzel, *Electrochim. Acta* **29**, 1305 (1984).
16. H. Schäfer, *Habilitationsschrift*, Universität Göttingen (1973).
17. I. Rubinstein, *J. electrochem. Soc.* **130**, 1509 (1983).
18. E. Gileadi, L. Duic and J. O'M. Bockris, *Electrochim. Acta* **13**, 1915 (1968).
19. P. Zelenay and J. Sobkowski, *Electrochim. Acta* **29**, 1715 (1984).
20. J. P. Hoare, *Adv. Electrochem.* **6**, 201 (1967).
21. F. Beck and H. Schulz, *Electrochim. Acta* **29**, 1569 (1984).
22. M. Fleischmann, K. Korinek and D. Pletcher, *J. electroanal. Chem.* **31**, 39 (1971).
23. M. Fleischmann, K. Korinek and D. Pletcher, *J. chem. Soc. Perkin Trans. II* 1396 (1972).
24. J. S. Clarke, R. E. Ehigamusoe and A. T. Kuhn, *J. electroanal. Chem.* **70**, 333 (1976).
25. F. Beck and W. Gabriel, *J. electroanal. Chem.* **182**, 355 (1985).
26. B. Wladislaw and H. Viertler, *J. chem. Soc. C*, 576, (1968).
27. E. Mageda, L. L. Miller and J. F. Wolf, *J. Am. chem. Soc.* **94**, 6812 (1972).
28. R. Lines and J. H. P. Utley, *J. chem. Soc., Perkin Trans. II*, 803 (1977).
29. J. W. Boyd, P. W. Schmalzl and L. L. Miller, *J. Am. chem. Soc.* **102**, 3856 (1980).
30. V. D. Parker, *J. chem. Soc. Chem. Commun.* 610 (1969).
31. T. Shono and Y. Matsamura, *J. Am. chem. Soc.* **91**, 2803 (1969).